Rheological characterization of sepiolite-vegetable oil suspensions at high pressures

M.J. Martín-Alfonso, A. Mejía, F.J. Martínez-Boza*, J.E. Martín-Alfonso

Centro de Investigación en Tecnología de Procesos y Productos Químicos. (Pro2Tecs). Escuela Técnica Superior de Ingeniería, Universidad de Huelva. Avda. Tres de Marzo s/n, Huelva (Spain)

Keywords: sepiolite, vegetable oil, drilling fluid, high-pressure

Corresponding author: martinez@uhu.es

Abstract

Drilling operations performed on geothermal wells require the ongoing search for sustainable fluids that will offer maximum performance and minimum environmental impact. Therefore, studies on the replacement of traditional clay suspensions in mineral and synthetic oils with clay suspensions in vegetable oils have offered some promising results. These preliminary results suggest the need for more extensive studies, including those considering high-pressure/high-temperature (HPHT) conditions, to assess the real capacity of biodegradable oils as substitutes for mineral and synthetic oils in oil-based muds (OBM) formulations.

This work analyses the structure and thermomechanical properties of commercial organo-sepiolites dispersed in vegetable oils, as a function of temperature and pressure. This serves as the principal criterion for the development of environmentally-friendly OBM for HPHT drilling applications. The results suggest that organo-sepiolites in vegetable oil suspensions have suitable thermal and mechanical properties to produce sustainable and environmentally-friendly drilling fluid for application at a wide range of temperatures and pressures.

1. Introduction

Deep well drilling and enhanced oil recovery (EOR) demand an ongoing search for suitable fluids to overcome the challenges associated with extreme temperatures and pressures under which these operations take place. At the same time, the reduction of the environmental impact associated with these activities is a major goal of the oil industry. One current trend used in response to these challenges is the development of sustainable and environmentally-friendly fluids having high efficiency and minimum cost (Apaleke et al., 2012).

Drilling fluids perform a variety of functions including the removal of cuttings, the stabilization of the wellbore and the lubrication of the drill bit. The viscous behaviour of drilling fluid is essential to ensure successful drilling operations, especially in the removal of drill cuttings. A suitable rheology is one of the most important properties of drilling fluids (high viscosity at low shear-rate, shear-thinning behaviour, and finite yield stress) to suspend and transfer drill cuttings to the surface (Caenn et al., 2017). Water-based muds (WBM) are preferable, from both an economic and environmental point of view (Amani et al., 2012; Reinoso et al., 2019, 2020). However, oil-based muds (OBM) have more suitable technical properties for aggressive environments, including high thermal stability, shale inhibition and lubricity (Khodja et al., 2010; Hermoso et al., 2015).

Sepiolite is a fibrous clay mineral which, due to its high aspect ratio, provides rheological improvements, similar to those of layered clays at lower concentrations. Sepiolite has been extensively used as a rheology improver and a fluid-loss controller in WBM. Guven et al. (1988) examined the rheology and fluid-loss properties of water-based drilling fluids made from distinct clays (bentonite, saponite and sepiolite) and their mixes. They concluded that fibrous sepiolite improves viscosity, gel strength and fluid-loss at high temperatures, even in the presence of common salts. Altun et al. (2015) tested water-based sepiolite suspensions for geothermal drilling, determining high resistance to salty environments in wells with high-pressure and high-temperature (HPHT). Huang et al. (2016) reported that sepiolite imparts time-dependent properties to water-based muds made of bentonite and sepiolite. Several authors have reported the beneficial effect of nano-size sepiolites as additives, improving both rheological properties and fluid-loss in water-based drilling fluids and bentonite muds (Abdo et al., 2016; Al-Malki et al., 2016).

Recently, OBM formulated with sepiolite have gained increasing attention (Zhuang et al., 2019). Zhuang et al. (2018a) studied both the structure of organo-sepiolite particles

(OSep) prepared with an ammonium salt and the rheological properties of OBM formulated with white oil as a function of surfactant content. The surfactant mainly covered the surface of the clay, improving compatibility oil-clay and rheological properties proportional to surfactant concentration. However, extremely high surfactant levels caused a decline in the rheological properties. Weng et al. (2018) prepared OSep with cationic and anionic surfactants and diesel oil. Cationic surfactants with long chains had better adhesion to the surface, but new cationic-anionic surfactants demonstrated the OBM's excellent thermal stability. The partial insertion of cationic surfactants in the sepiolite's channel resulted in improved rheological and thermal stability (Zhuang et al., 2018b). The synergetic effect between fibrous sepiolite and layered montmorillonite has been also assessed, concluding that the resulting structural reinforcement leads to improved rheological properties and thermal stability in the OBM (Zhuang et al., 2018c).

To face the current challenge of environmental sustainability, mineral and synthetic oils can be replaced by vegetable oils (Tapavicza, 2015). Very few studies have been carried out using vegetable oil-based formulations. Agwu et al. (2015) studied both rheological and fluid-loss properties of oil-based muds formulated with soybean oil. These muds displayed Bingham plastic flow behaviour with low yield stress. Density and fluid-loss properties were similar to those of diesel oil muds. Sulaimon et al. (2017) compared the rheological behaviour, filtration characteristics and emulsion stability of oil-based muds formulated with palm methyl ester with samples of synthetic oil-based muds, based on the API viscosity requirement. They concluded that the emulsion must be optimized to reduce viscosity and fluid-loss. Li et al. (2016) concluded that biodiesel-based drilling fluid is a valuable alternative for further OBM development.

Ratkievicius et al. (2017) examined OBM formulated with bentonite and soybean oil, demonstrating that surface modification of the clay enhanced its ability to serve as a

viscosity improver in a soybean oil-based drilling fluid. Surfactant concentration, however, was found to be of little relevance.

These promising results suggested that more extensive studies, including those examining HPHT conditions, need to be performed to assess the actual capacity of biodegradable oils to substitute mineral and synthetic oils in OBM formulations.

Therefore, this work examines the rheological behaviour of commercial organo-sepiolites dispersed in vegetable oils, as a function of temperature and pressure, as the principal criterion for developing environmentally-friendly OBM for HPHT drilling applications.

2. Experimental

2.1 Materials and methods

Crude vegetable oils from sunflower (SC) and rape (RC) were provided by LIPSA (Spain) with no additional modifications made in the preparation of the oil-based suspensions.

Raw sepiolite (Sep) and two commercial organo-sepiolites (OSepSB5 and OSepSB20, with brand names Berkbent SB-5 and Berkbent SB-20, respectively) were donated by TOLSA (Spain). According to the supplier, both OSepSB5 and OSepSB20 were obtained from Sep through surface modification with an alkyl ammonium cationic surfactant. OSepSB5 fibres are less polar than OSepSB20 and they would be more compatible with non-polar solvents.

Sepiolite suspensions were prepared by mixing organoclays (at a concentration of 3 wt%) in a vegetable oil base using an Ultra-Turrax high-performance dispersing machine (Ika, Germany) at 60ºC and 9000 rpm for five minutes. Prior to the high shear processing, organoclays were wetted with the oil in a low shear mixer, using a conventional four-blade impeller, at room temperature, for two hours. The suspensions were stored in closed

containers at room temperature. Before the testing samples were homogenised in a low shear mixer for five minutes, no separation phase was observed.

2.2 Thermogravimetric analysis

Thermogravimetric analyses were performed using a TGA (TA Instrument) under N_2 flow, for 5-15 mg of each sample. Oil-based samples were isothermally stabilized at 55ºC for five minutes and were subsequently heated to 600ºC at a 20ºC·min^{-1} heating rate.

2.3 Calorimetric analysis

Calorimetric analyses were carried out using an MDSC (TA Instrument) with 5-15 mg of each sample in sealed aluminium pans, purged with N_2 at 50 mL/min. An oscillation period of 60 seconds, an amplitude of 0.50°C, and a heating rate of 5°C/min were used. Temperatures ranged from -80 to 250°C.

2.4 X-Ray Diffraction

XRD measurements were taken at room temperature, using a Bruker S8 Advance diffractometer (Germany) equipped with a secondary monochromator, a Brentano Bragg geometry goniometer and a copper cathode as an X-ray source. Samples were subjected to Cu Kα radiation with a wavelength of 0.15406 nm. The 2θ angles ranged from 1.5º to 40º, with a 0.017º single scanning step and a measurement time of 6 seconds per step.

2.5 SEM

Suspension morphologies were observed with a Jeol JSM-5410 scanning electron microscope (20 kV and 10,000x), using samples coated with gold at high vacuum to avoid charging. The excess of oil was removed by absorption on cellulose paper and further by high vacuum before metallisation.

2.6 Rheological characterization

Rheological measurements were taken using a controlled-stress rheometer (Haake Mars II, Thermo Scientific). Rheological data were obtained at atmospheric pressure using standard coaxial cylinder geometry (DINZ20). Pressure–temperature data were obtained using a non-conventional coaxial cylinder-type pressure cell (HP2000) designed in our laboratory. It was equipped with a magnetically-coupled coaxial cylinder (26 mm and 28 mm inner and outer diameter, respectively) having a length of 80 mm.

Steady-state flow curves were measured at distinct temperature and pressure combinations (20ºC, 40ºC, 60ºC, 80ºC and 100ºC and 1 bar, 500 bar, 1000 bar, 1500 bar), using an upward and downward stress sweep test, in 180-second steps. Differences observed between upward and downward curves were considered to be within the experimental error range of ±5%.

Viscosity versus pressure ramps were measured at 20ºC, 40ºC, 60ºC, 80ºC and 100ºC, at a fixed shear-rate of 900 s^{-1}, increasing/decreasing pressure at 10 bar/min, using a high-pressure generator (HiP, USA). The sample itself was used as a pressurizing fluid. No significant hysteresis was observed when comparing upward and downward pressure sweeps.

3. Results and discussion

3.1 Thermomechanical characterization

As Figure 1 shows, Sep had a weight loss of 7.21% at room temperature to 150ºC, caused by surface water loss. The loss of zeolitic and structural water occurs in two stages: from 150ºC to 320ºC, with 2.69% weight loss, and from 320ºC to 595ºC, with 2.22% weight loss (Tartaglione et al., 2008; Tiemblo et al., 2015).

Weight loss due to a decrease in surface water for OSepSB5 and OSepSB20 at room temperature to 150ºC was 5.1% and 5.87%, respectively. These values of weight loss

seem to be high for surface water if the hydrophobic surface is homogeneously covered. In this case, water could be between the clay surface and the headgroup of the surfactant. Assuming that the surfactant is stable at temperatures below 150ºC, less surface water is adsorbed on OSep due to the partial covering of the surface by surfactants, as has been previously noted (Weng et al., 2018; Zhuang et al., 2018b). Both the loss of structural water and the decomposition of the surfactant take place in superposed stages in the 150ºC-320ºC interval, with weight losses of 5.98% and 4.00% for OSepSB5 and OSepSB20, respectively, and in the 320ºC-595ºC interval, with weight losses of 8.68% and 9.09% for OSepSB5 and OSepSB20, respectively.

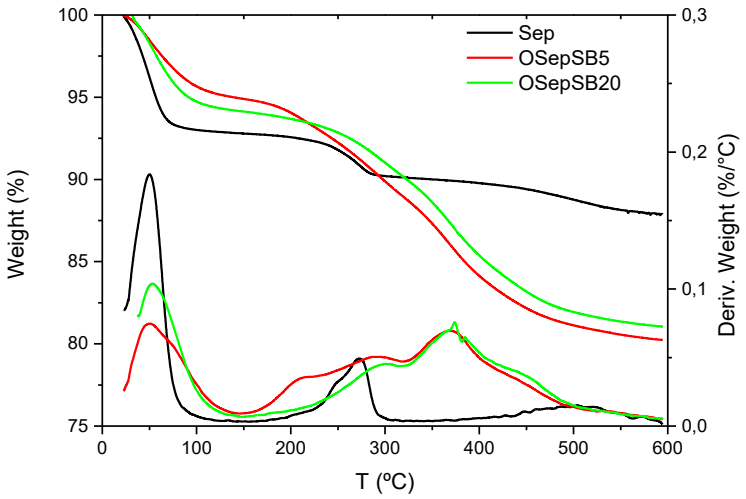

Figure 1. TGA thermograms for raw Sep, OSepSB5 and OSepSB20.

Based on these results, the water content of dry Sep is estimated at 5.59 g/100 g. Therefore, surfactant content may be estimated at 12% for the OSepSB5 sample and 10% for the OSepSB20 sample (García-López et al., 2010) if a similar mechanism occurs in the organoclay for the dehydration process.

Figure 2 shows the thermogram of the base oils and OBM formulated with 3 wt% of OSep. As Figure 2 reveals, both vegetable oils and OSep suspensions have high thermal resistance. Sunflower and rape vegetable oil samples have a weight loss of 1% at 279.3ºC

and 279.5ºC, respectively. Suspensions have a weight loss of 1% at lower temperatures than the respective vegetable oil, at 239.9ºC and 237.2ºC for OSepSB5 and OSepSB20 in sunflower oil and 255.3ºC and 268.3ºC for OSepSB5 and OSepSB20 in rape oil, respectively. These results may be explained by the combined effect of weight loss due to water dehydration and the incipient surfactant decomposition. A 5% weight loss takes place at temperatures of 369.8ºC, 351.9ºC and 347.0ºC for sunflower oil, OSepSB5_SC and OSepSB20_SC suspensions, and 366.7ºC, 352.3ºC and 360.2ºC for rape oil, OSepSB5_RC and OSepSB20_RC suspensions, respectively. According to these results, rape suspensions appear to be slightly more resistant to thermal decomposition than sunflower suspensions.

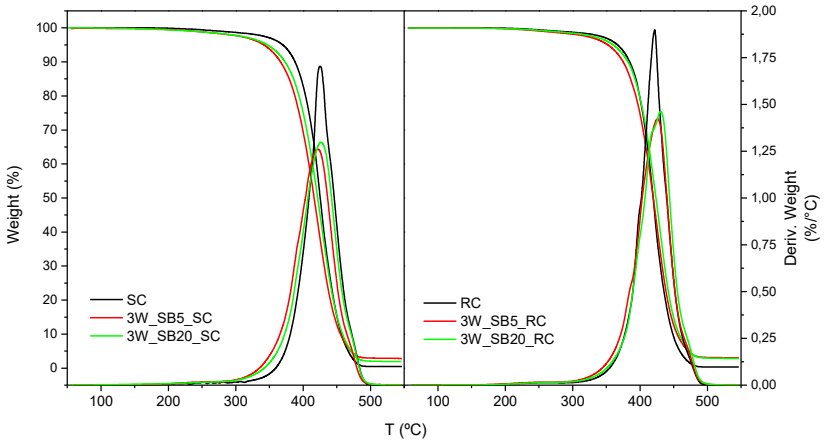

Figure 2. TGA thermograms of vegetable oils and OSep suspensions.

Figure 3 shows the DSC cooling curves for the examined suspensions. Sunflower oil reveals extensive exothermic crystallization with three characteristic events: cloud point at -9.2ºC with the onset of the first peak related to the incipient crystallization of higher molecular weight waxes; a first crystallization peak (pk1) at -19ºC related to microcrystal formation; and a second peak (pk2) at -42.2ºC related to recrystallizations and the arrangements of microcrystal to form polymorphic structures (Chapman, 1963; Adhvaryu

et al., 2003). Rape oil has similar cooling endotherms with a cloud point and crystallization peaks at lower temperatures (-13.5ºC, -24.0ºC and -55.4ºC for onset, pk1 and pk2, respectively).

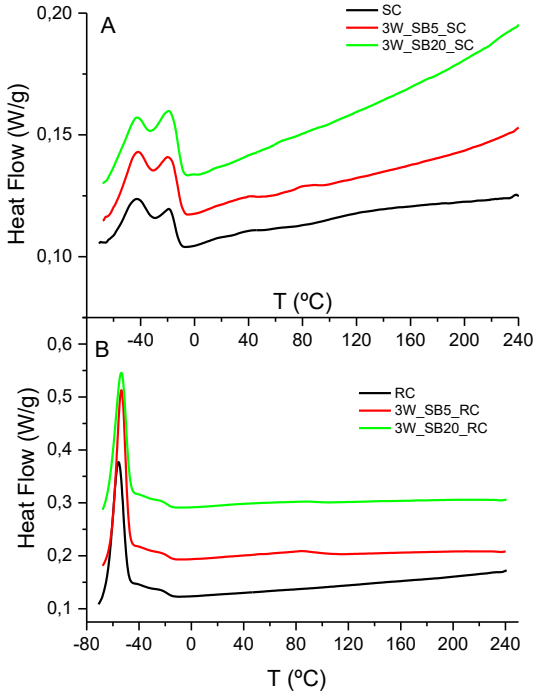

Figure 3. Cooling curves from DSC for the examined vegetable oils and suspensions.

The OBM under study revealed very similar characteristic crystallization events as those of the corresponding base oil, with minimal differences in onset and peak temperatures (±1ºC). The OBM formulations with different types of organoclay (OSepSB5 and OSepSB20) do not reveal distinct crystallization curve shapes or thermal event temperatures. This suggests that these OSep do not act as nucleating agents for oil crystallization. The thermal properties of drilling muds formulated with vegetable oils and organo-sepiolites appear to depend primarily on the characteristics of the base oil. According to the results of the DSC and TGA, these muds may be potentially used at a wide range of temperatures, from -10ºC to 245ºC.

3.2 Structural characterization

The XRD patterns of raw sepiolite, OSep and the prepared oil-based muds are presented in Figure 4. The XRD patterns of OSep and their suspensions are very similar to the pattern found for Sep. Main reflections in Sep that appear at 2θ values of 7.4º; 11.7º; 13.3º; 19.8º; 20.6º; 23.8º; 26.7º and 35º, also appear in OSep. This has been previously noted by several authors (García-López et al., 2010; Weng et al., 2018; Zhuang et al., 2018a, 2018b), indicating that surfactant modification does not affect the crystalline structure of Sep, due to the covalent linkages between sheets. On the other hand, the absence of additional reflections in OSep samples appears to indicate that surface amorphous adsorption of the surfactant is the predominant mechanism for organic modification, regardless of the type of organic surfactant.

The presence of vegetable oil increases the intensity in the 2θ 17º-24º range, regardless of the oil source (sunflower or rape). Similar results were reported by Zhuang et al. (2018a) for drilling fluids made from synthetic white oil and organo-sepiolites. These results suggest that the amorphous adsorption of the oil phase of the mud is the predominant mechanism for oil and organoclay interaction. No additional influence in either the nature or type of oil has been observed in the XRD, except for a decreased intensity of the reflections at high values of 2θ (35º) taking place in all suspensions. Consequently, as found by Zhuang et al. (2018a), there were no significant changes observed in the crystalline structure of OSep based on the type of alkyl ammonium salt used for modification.

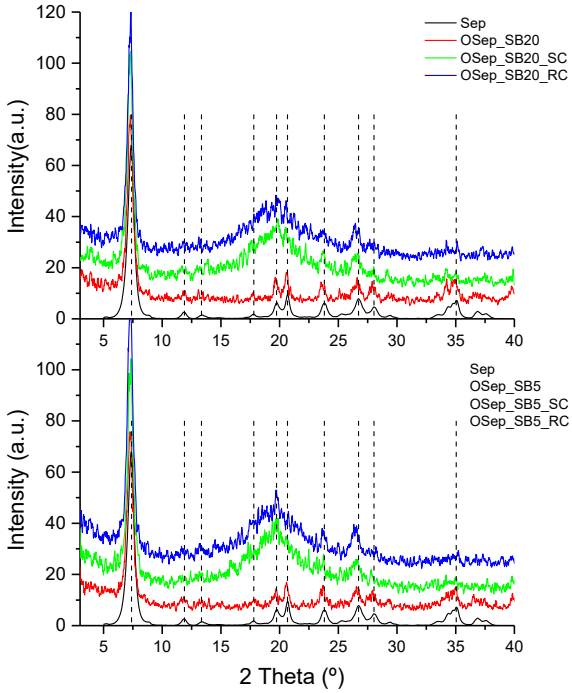

Figure 4. XRD patterns of raw sepiolite (Sep), organo-sepiolites (OSepSB5 and OSepSB20) and suspensions in sunflower and rapeseed vegetable oils (OSepSB5_SC; OSepSB20_SC; OSepSB5_RC; OSepSB20_RC).

Figure 5 shows the SEM surface morphology of OSep and their suspensions in sunflower oil after being submitted to a large vacuum for metalation. Both OSep samples (OSepSB5 [Figure 6A] and OSepSB20 [Figure 6B]) have the characteristic morphology of fibrous aggregates, similar to that previously found by other authors (García-López et al., 2010; Abbho et al., 2016; Zhuang et al., 2017, 2018). The presence of sunflower vegetable oil separates the aggregates, creating a "spaghetti-like" morphology that is more homogeneous in OSepSB20. This would explain the increased stability observed for the OSepSB20 suspension in vegetable oil. Thus, the rheological study focused on the OSepSB20 suspension.

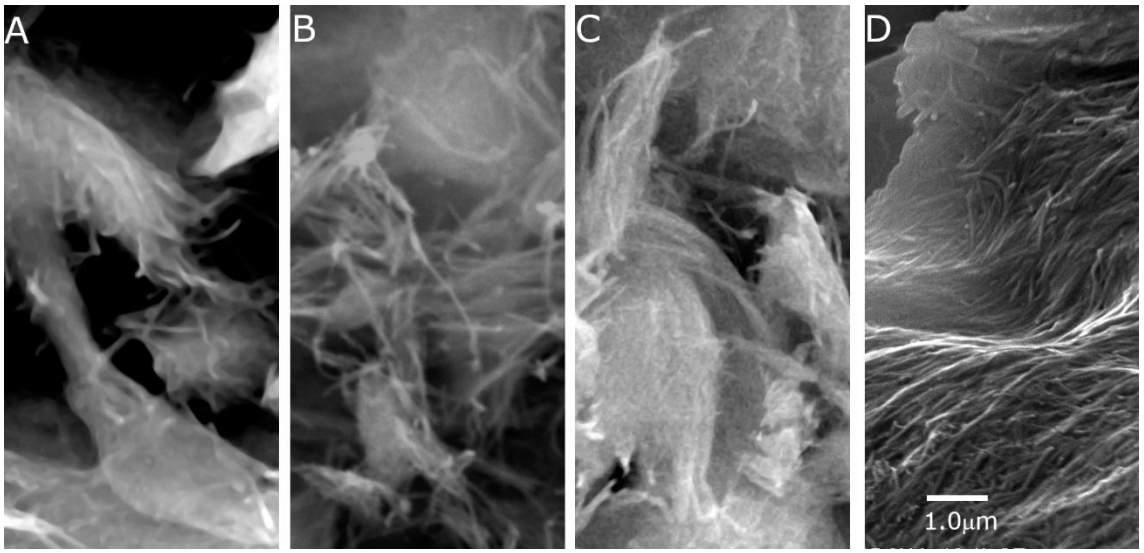

Figure 5. SEM images. A) OSepSB5; B) OSepSB5_SC; C) OSepSB20; and D) OSepSB20_SC.

3.3 Rheological characterization

Figures 6 and 7 show the steady-state flow curves for the suspensions studied in the 20ºC -100ºC range, at pressures of 1 and 1000 bar, respectively. In general, these suspensions demonstrate pseudoplastic behaviour in the studied shear-rate range. In the low shear-rate region, interactions between OClay particles dispersed in the Newtonian oil medium lead to a weak structure of connected aggregates, with high viscosity values and a low apparent yield stress. This behaviour is characteristic of OClay in oil suspensions above a threshold concentration, approximately 3 wt%, as previously demonstrated (Hermoso et al., 2014a, 2014b) As the shear-rate increases, the dispersion structure progressively disappears. The orientation of the OClay in the flow direction leads to a decrease in the degree of the interactions in the dispersed phase with the resulting decrease in viscosity. Further, at a higher shear-rate, the suspension shows a tendency to reach a limiting value of the viscosity, significantly higher than that of the continuous phase formed by the Newtonian oil. In this region, the viscosity of the suspension depends mainly on the concentration of

particles since a maximum orientation of the particles under flow results in a minimum degree of interactions between the dispersed OClay particles. The main contribution of pressure is the increased bulk viscosity of the continuous oil phase, as seen when comparing Figures 6 and 7. In addition, the pressure slightly alters the system's pseudoplastic behaviour, as discussed below.

This shear-thinning behaviour is useful for drilling mud in which a high viscosity, at low shear-rate, prevents the settling process of the cutting when the circulation of the fluid is stopped. In contrast, a low viscosity at higher shear-rates saves energy and increases the rate of penetration of the bit. In this sense, these OSep in vegetable oil suspensions demonstrate suitable properties as rheology modifiers for drilling fluids, given their higher viscosity values in the low shear-rate region at near resting conditions, and their lower viscosity values in high shear-rate regions, due to the alignment of OSep fibres under flow.

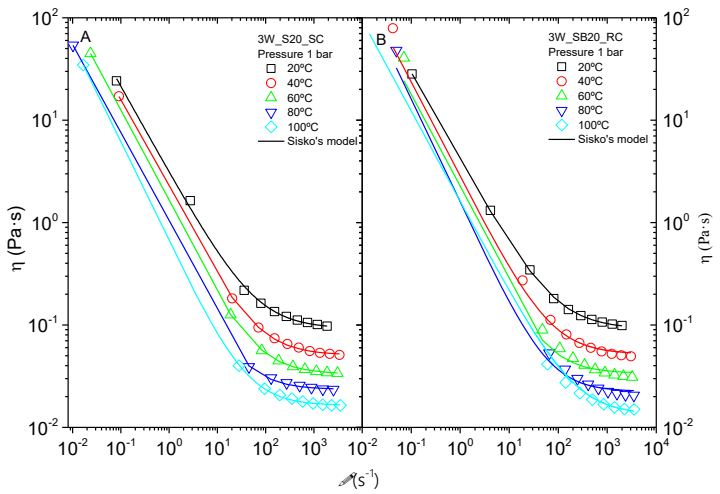

Figure 6. Steady state flow curves, at atmospheric pressure, as a function of temperature, for OBM formulated with 3 wt% of OSepSB20. A) Suspension in sunflower oil (3W_SB20_SC); B) Suspension in rapeseed oil (3W_SB20_RC).

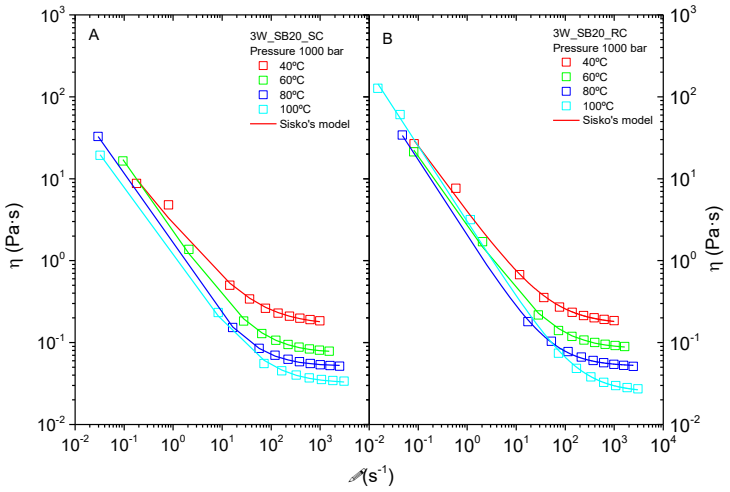

Figure 7. Steady state flow curves, at a pressure of 1000 bar, as a function of temperature, for OBM formulated with 3 wt% of OSepSB20. A) Suspension in sunflower oil (3W_SB20_SC); B) Suspension in rapeseed oil (3W_SB20_RC).

At ambient pressure and constant temperature, the viscous flow behaviour of OSep suspensions can be modelled by the classic Sisko's model:

$$\eta = \eta_{\infty} + k_0 \cdot \dot{\gamma}^{n_0 - 1} \qquad (1)$$

Where η_{∞} is the high-shear-rate-limiting viscosity, k_0, is the consistency index, n_o is the flow index and $\dot{\gamma}$ the shear-rate. As Figure 6 reveals, Sisko's model satisfactorily describes the flow behaviour of both suspensions in the examined temperature range. As expected, higher viscosity values are obtained at low temperatures. An increased temperature leads to a decreased viscosity for OSep suspensions in both oils. Pressure has the opposite effect of temperature, with viscosity increasing as pressure increases for all temperatures tested, but to a lower extent than the decreases observed with the temperature increases. In addition, the effect of temperature is dampened at high pressure, as observed when comparing Figures 6 and 7.

As previously mentioned (Hermoso et al., 2014a), Sisko's model can be generalised to include the effect of pressure on the flow behaviour of both the continuous and dispersed suspension phases, at a constant temperature, obtaining the generalised Sisko-Barus' model.

$$\eta = \left(\eta_{\infty} + (k_0 + k_1(P - P_r)) \cdot \dot{\gamma}^{(n_0 + n_1(P - P_r)) - 1}\right) \exp\left(\beta_o(P - P_r) + \beta_1(P - P_r)^2\right) \quad (2)$$

Where k_1 and n_1 are fitting parameters that assess the effect of pressure on consistency and flow indexes of the classic Sisko's model (Eq. 1), respectively. β_o is the Barus' piezoviscous coefficient, at a constant temperature; β_1 is a fitting parameter that corrects the deviation of the Barus' piezoviscous coefficient when the system is studied at higher pressures; *P* and *Pr* are the applied and reference pressure, respectively. In this approach, the effect of pressure is separated into two main contributions. Firstly, the generalised Barus' equation would assess the contribution of pressure to the bulk viscosity of the system under flow. Therefore, the values of β_o and β_1 have been obtained by fitting the viscosity-pressure data measured at a constant shear-rate and temperature in the high shear-rate region (see Figure 7).

Parameters k_1 and n_1 would modulate the effect of pressure, previously assessed by the generalised Barus' model, over the pseudoplastic decrease in the intermediate and low shear-rate regions. Thus, parameters k_1, n_1 and η_{∞} have been obtained by fitting the flow curves to the generalized Sisko-Barus' measured in the 20ºC -100ºC temperature range and at 1-1500 bar of pressure, with a fixed β_o and β_1. The values of the parameter of Sisko's model are shown in Table I and II for sunflower and rape oil-based suspensions, respectively.

As observed, the set consistency, flow indexes and limiting viscosity of Sisko's model (Eq. 1) decrease with temperature for both suspensions, due to the influence of the

Brownian motion on the suspension's degree of flocculation. Similarly, the piezoviscous coefficients decrease with temperature, with very similar values for both suspensions.

Table I. Parameters of the generalised Sisko's model for suspension based on sunflower vegetable oil.

	20ºC	40ºC	60ºC	80ºC	100ºC
k_o (s)	2.70	1.79	1.26	$4.74 \cdot 10^{-01}$	$5.82 \cdot 10^{-01}$
k_1 (s/bar)	$-1.50 \cdot 10^{-03}$	$-1.02 \cdot 10^{-03}$	$-4.68 \cdot 10^{-04}$	$-3.32 \cdot 10^{-05}$	$-1.17 \cdot 10^{-04}$
n_o	$1.41 \cdot 10^{-01}$	$1.16 \cdot 10^{-01}$	$8.82 \cdot 10^{-02}$	$6.49 \cdot 10^{-02}$	$7.02 \cdot 10^{-02}$
n_1 (bar^{-1})	$3.32 \cdot 10^{-05}$	$1.31 \cdot 10^{-04}$	$1.70 \cdot 10^{-05}$	$3.35 \cdot 10^{-05}$	$2.23 \cdot 10^{-05}$
$\eta\infty$ (Pa·s)	$9.87 \cdot 10^{-02}$	$5.03 \cdot 10^{-02}$	$2.87 \cdot 10^{-02}$	$2.19 \cdot 10^{-02}$	$1.56 \cdot 10^{-02}$
β_o (bar)	$1.44 \cdot 10^{-03}$	$1.32 \cdot 10^{-03}$	$1.06 \cdot 10^{-03}$	$9.42 \cdot 10^{-04}$	$8.15 \cdot 10^{-04}$
β_1 (bar^{-2})	$-1.58 \cdot 10^{-07}$	$-1.17 \cdot 10^{-07}$	$-5.11 \cdot 10^{-08}$	$-4.01 \cdot 10^{-08}$	$-2.22 \cdot 10^{-08}$
Pr (bar)	1	1	1	1	1

Table II. Parameters of the generalised Sisko's model for suspension based on rapeseed vegetable oil.

	20ºC	40ºC	60ºC	80ºC	100ºC
k_o (s)	3.81	2.63·	1.45·	1.49	2.33
k_1 (s/bar)	$-2.48 \cdot 10^{-03}$	$-1.48 \cdot 10^{-03}$	$-5.09 \cdot 10^{-04}$	$-5.92 \cdot 10^{-04}$	$-8.97 \cdot 10^{-04}$
n_o	$1.61 \cdot 10^{-01}$	$7.07 \cdot 10^{-02}$	$7.91 \cdot 10^{-02}$	$1.01 \cdot 10^{-02}$	$3.00 \cdot 10^{-02}$
n_1 (bar^{-1})	$-4.81 \cdot 10^{-05}$	$1.12 \cdot 10^{-04}$	$4.85 \cdot 10^{-05}$	$6.50 \cdot 10^{-05}$	$2.92 \cdot 10^{-05}$
$\eta\infty$ (Pa·s)	$9.12 \cdot 10^{-02}$	$5.14 \cdot 10^{-02}$	$3.17 \cdot 10^{-02}$	$2.14 \cdot 10^{-02}$	$1.26 \cdot 10^{-02}$
β_o (bar)	$1.55 \cdot 10^{-03}$	$1.30 \cdot 10^{-03}$	$1.07 \cdot 10^{-03}$	$9.15 \cdot 10^{-04}$	$7.52 \cdot 10^{-04}$
β_1 (bar^{-2})	$-2.54 \cdot 10^{-07}$	$-1.15 \cdot 10^{-07}$	$-6.07 \cdot 10^{-08}$	$-4.08 \cdot 10^{-08}$	$-1.98 \cdot 10^{-08}$
Pr (bar)	1	1	1	1	1

Pressure slightly decreases the sensitivity to shear of these OSep suspensions in vegetable oil. On the one hand, the pseudoplastic decline flattens to the limiting value at lower shear-rates, as deduced from the negative value of the k_1 parameter. Thus, the consistency index decreases when pressure increases, at a constant temperature, for all temperatures tested. On the other hand, the flow indexes increase with pressure (positive value of parameter n_1), flattening the slope of the pseudoplastic decline as pressure increases, as seen in Figure 8. Similar behaviour was observed by the authors for the oil-based drilling fluid formulated with organobentonites in mineral oil (Hermoso et al., 2014a). These results indicate that the interaction between particles in the suspension are favoured at low temperatures and high pressures.

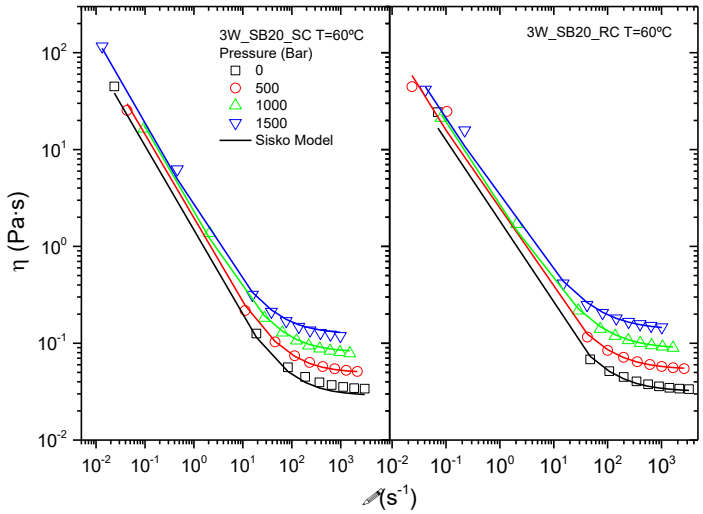

Figure 8. Steady state flow curves, at 60ºC, as a function of the pressure, for OBM formulated with 3 wt% of OSepSB20. A) Suspension in sunflower oil (3W_SB20_SC); B) Suspension in rapeseed oil (3W_SB20_RC).

To model the viscosity-pressure behaviour at high circulation shear-rates, viscosity-pressure curves were measured at a constant shear-rate of 900 s^{-1}. The results for the OSepSB20 suspensions are presented in Figure 9.

As observed, the viscosity at high shear-rates increases with pressure, with a progressive negative deviation from linearity in log scale being found at higher pressures. Therefore, the extrapolation of the pressure behaviour based on the exponential Barus' model leads to an overestimation of the effect of pressure on the high-pressure region and should be corrected by a quadratic parameter β_1 (see Table I and II). In the high shear-rate region the effect of pressure on the viscosity of both OSep suspensions is very similar to those of its respective Newtonian vegetable oil. This observation indicates that viscosity-pressure behaviour in this region mainly depends on the piezoviscous properties of the continuous phase, being the influence of the dispersed phase less significant, as has been previously reported for organo-bentonite suspensions (Hermoso et al., 2014a).

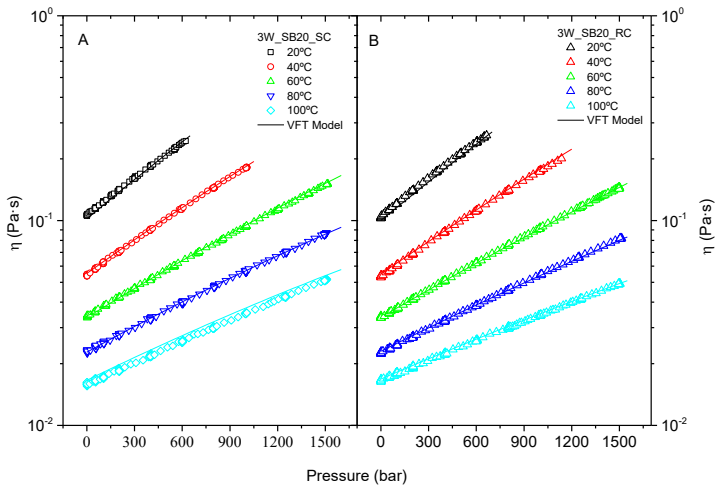

Figure 9. Viscosity-pressure curves, as a function of temperature, measured at 900 s^{-1}, for OBM formulated with 3 wt% of OSep. SB20. A) Suspension in sunflower oil (3W_SB20_SC); B) Suspension in rapeseed oil (3W_SB20_RC).

In addition, the viscosity-pressure-temperature behaviour has been modelled using the VFT equation:

$$\eta = A \cdot exp\left(a_1(P - P_r) + a_2(P - P_r)^2 + \frac{(B + b_1(P - P_r) + b_2(P - P_r)^2 + b_3(P - P_r)^3)}{T - C}\right) \quad (3)$$

Where A, B and C are parameters of Vogel's model and a_1, a_2, b_1, b_2 and b_3 are empirical parameters that consider the effect of pressure. Parameter values for the analysed samples are presented in Table III. VFT equation may be a valuable engineering tool to generalize the viscosity-pressure-temperature behaviour over a wide range of temperatures and pressures, even better than other factorial models such as the WLF-Barus' model (Hermoso et al., 2014a), which requires additional fitting parameters.

Figure 10 shows the modelled viscosity-pressure-temperature data from viscosity-pressure tests, at 900 s^{-1}, compared to viscosity values, at the same shear-rate, obtained from the generalised Sisko-Barus' model using steady state data. A suitable agreement between the data from different tests is observed for all analysed samples. Viscosities of both sunflower and rapeseed oils have been included as references.

Table III. Parameters of the VTF model for the analysed samples.

	Sunflower oil	Rape oil	3W_SB20_SC Mud	3W_SB20_RC Mud
A/ Pa·s	$1.07 \cdot 10^{-04}$	$7.72 \cdot 10^{-05}$	$7.30 \cdot 10^{-04}$	$7.31 \cdot 10^{-04}$
B/ ºC	$1.03 \cdot 10^{+03}$	$1.15 \cdot 10^{+03}$	$6.66 \cdot 10^{+02}$	$6.79 \cdot 10^{+02}$
C/ ºC	$-1.40 \cdot 10^{+02}$	$-1.48 \cdot 10^{+02}$	$-1.14 \cdot 10^{+02}$	$-1.17 \cdot 10^{+02}$
a_1/ bar^{-1}	$-8.15 \cdot 10^{-04}$	$-8.98 \cdot 10^{-04}$	$-3.26 \cdot 10^{-04}$	$-4.52 \cdot 10^{-04}$
a_2/ bar^{-2}	0	0	0	0
b_1/ ºC·bar^{-1}	$3.68 \cdot 10^{-01}$	$4.10 \cdot 10^{-01}$	$2.39 \cdot 10^{-01}$	$2.64 \cdot 10^{-01}$

b_2/ ºC·bar^{-2}	-7.46·10^{-06}	-1.05·10^{-05}	-5.92·10^{-06}	-7.56·10^{-06}
b_3/ ºC·bar^{-3}	0	0	0	0
P_r/ bar	1	1	1	1

As observed in Figure 10, rapeseed oil has slightly higher viscosity values than sunflower oil in the overall range of temperatures tested. OSep suspensions prepared in both vegetable oils reveal a significant increase in viscosity as compared to the respective oil. This increase is more noticeable in the higher temperature regions, where the degree of deflocculation of the dispersed phase of OSep in the oil medium is favoured at high temperatures by the increased effective volume fraction (Wu et al., 2012). Therefore, the suspension shows a reduction of thermal susceptibility with respect to the vegetable oil at atmospheric pressure. Pressure leads to a reduction of the effective volume fraction, increasing the flocculation of OSep particles and reducing the contribution of the dispersed phase to the bulk properties of the suspension. Therefore, thermal susceptibility at high pressures is mainly determined by the continuous phase, being very similar to that of the respective oil.

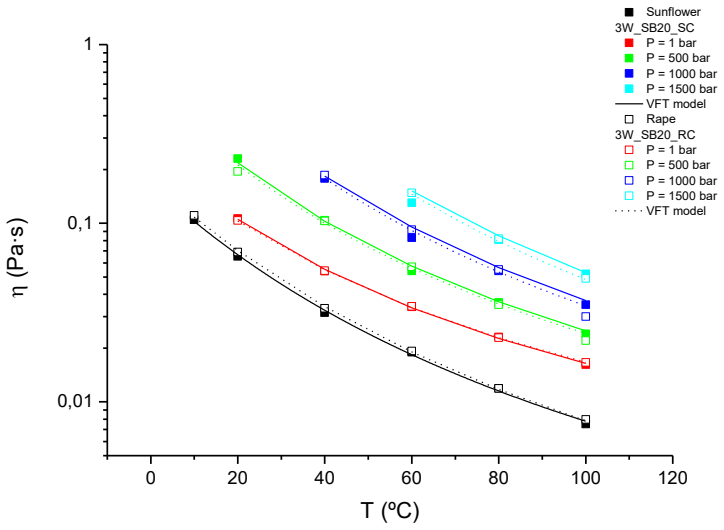

Figure 10. Evolution of the viscosity, at 900 s^{-1}, with temperature at selected pressures, for the analysed samples.

4. Conclusions

In this study, the structure and properties of organo-sepiolite suspensions in vegetable oil have been assessed. Thermal analysis reveals that these suspensions can be used as OBM in a wide range of temperatures, from higher than that of the on-set of the oil crystallization temperature (-10ºC) to lower than the initial surfactant decomposition temperature (240ºC). Suspensions made with rapeseed oil are slightly more resistant to thermal degradation than those made with sunflower oil.

These organo-sepiolites in vegetable oil suspensions have a fibrous structure due to the surface modification of the clay with no alteration of the crystalline structure. The fibrous structure is more developed for OSepSB20. This morphology leads to suitable rheological properties in drilling fluids, demonstrating a shear-tinning behaviour in a wide range of temperatures and pressures. The flow behaviour can be satisfactorily modelled with a modified Sisko's model. Both temperature and pressure decrease the shear-thinning properties of the suspensions, dampening the pseudoplastic decline regardless of the type of oil used.

Pressure and temperature have the opposed effect on viscosity, with the decreases caused by temperature being more significant. Nevertheless, the effect of temperature is dampened at high pressures with a reduction of thermal susceptibility with respect to atmospheric pressure. The viscosity at high shear-rates increases with pressure, demonstrating a progressive negative deviation of the exponential Barus' model. The

VFT equation satisfactorily models the viscosity-pressure-temperature behaviour at a high shear-rate in the overall experimental design.

Authors contributions

M.J. Martín-Alfonso and A. Mejía carried out the experiments and data analysis. M.J. Martín-Alfonso contributed to the interpretation of the results. F. J. Martínez-Boza wrote the manuscript with support from M. J. Martín-Alfonso and J.E Martín-Alfonso.

Declaration of Competing Interest

None.

Acknowledgements

This work was supported by FEDER (grant numbers CTQ-2017-89792-R, P18-RT-4684 and AT17_5978).

5. References

Abdo, J., Al-Sharji, H., Hassan, E., 2016. Effects of nano-sepiolite on rheological properties and filtration loss of water-based drilling fluids. Surf. Interface Anal. 48, 522-526. https://doi.org/10.1002/sia.5997

Adhvaryu, A., Erhan, S., Perez, J., 2002. Wax appearance temperatures of vegetable oils determined by differential scanning calorimetry: effect of triacylglycerol structure and its modification. Thermochim. Acta. 395(1), 191–200. https://doi.org/10.1016/S0040-6031(02)00180-6

Agwu, O.E.; Okon, A.N., Udoh, F.D., 2015. A Comparative Study of Diesel Oil and Soybean Oil as Oil-Based Drilling Mud. J. Petrol. Eng. ID 828451. http://dx.doi.org/10.1155/2015/828451

Al-Malki, N., Pourafshary, P., Al-Hadrami, H., Abdo, J., 2016. Controlling bentonite-based drilling mud properties using sepiolite nanoparticles. Petrol. Explor. Develop. 43(4), 717-723.

Altun, G., Osgouei, A.E., Ozyurtkan, M.H., 2015. Sepiolite based muds as an alternate drilling fluid for hot environments. Proceedings of the 2015 World Geothermal Congress. Melbourne, Australia, 19-25 April 2015.

Amani, M., Al-Jubouri, M., Shadravan, A., 2012. Comparative Study of Using Oil-Based Mud Versus Water-Based Mud in HPHT Fields. Advances in Petroleum Exploration and Development. 4(2): p. 18-27. http://dx.doi.org/10.3968/j.aped.1925543820120402.987.

Apaleke, A.S., Al-Majed, A.A., Hossain, M.E., 2012. Drilling Fluid: State of The Art and Future Trend. In North Africa Technical Conference and Exhibition. Society of Petroleum Engineers. https://doi.org/10.2118/153676-MS.

Caenn, R., Darley, H.C.H., Gray, G.R., 2017. Composition and Properties of Drilling Fluids and Completion Fluids 7th ed. Gulf Professional Publishing, Houston.

Chapman D., 1962. The polymorphism of glycerides. Chem. Rev. 62, 433.

García-López, D., Fernández, J.F., Merino, J.C., Santarén, J., Pastor, J.M., 2010. Effect of organic modification of sepiolite for PA 6 polymer/organoclay nanocomposites. Compos. Sci. Technol. 70, 1429 - 1436. http://dx.doi.org/10.1016/j.compscitech.2010.05.020.

Guven, N., Panfil, D.J., Carney, L.L., 1988. Comparative Rheology of Water-Based Drilling Fluids With Various Clays. International Meeting on Petroleum Engineering, SPE-17571-MS.DOI. https://doi.org/10.2118/17571-MS.

Hermoso, J., Martínez-Boza, F., Gallegos, C., 2014a. Influence of viscosity modifier nature and concentration on the viscous flow behavior of oil-based drilling fluids at high pressure. Appl. Clay Sci. 87, 14-21. http://dx.doi.org/10.1016/j.clay.2013.10.011.

Hermoso, J., Martínez-Boza, F., Gallegos, C., 2014b. Combined effect of pressure and temperature on the viscous behaviour of all-oil drilling fluids. Oil Gas Sci. Technol. 69(7), 1283-1296. http://dx.doi.org/10.2516/ogst/2014003.

Hermoso, J., Martínez-Boza, F., Gallegos, C., 2015. Influence of aqueous phase volume fraction, organoclay concentration and pressure on invert-emulsion oil muds rheology. J. Ind. and Eng. Chem. 22, 341-349. http://dx.doi.org/10.1016/j.jiec.2014.07.028.

Huang, W., Leong, Y., Chen, T., Au, P., Liu, X., Qiu, Z., 2016. Surface chemistry and rheological properties of API bentonite drilling fluid: pH effect, yield stress, zeta potential and ageing behaviour. J. Pet. Sci. Eng. 146, 561–569. https://doi.org/10.1016/j.petrol.2016.07.016

Khodja, M., Canselier, J. P. ,Bergaya, F, Fourar, K., d, Khodja, M.,

Li, W., Zhao, X., Ji, Y., Peng, H., Li, Y., Liu, L., Han, X. 2016. An investigation on environmentally friendly biodiesel-based invert emulsion drilling fluid. J Petrol Explor Prod Technol (2016) 6:505–517. https://doi.org/10.1007/s13202-015-0205-7.

Man, Y., Tan, C., 2002. Comparative differential scanning calorimetric analysis of vegetable oils: II. Effects of cooling rate variation. Phytochem. Anal. 13(3), 142–151. https://doi.org/10.1002/pca.634

Ratkievicius, L., Filho, F., Neto, E., Santanna, V., 2016. Modification of bentonite clay by a cationic surfactant to be used as a viscosity enhancer in vegetable-oil-based drilling fluid. Appl. Clay Sci. 135,307-312. http://dx.doi.org/10.1016/j.clay.2016.10.011.

Reinoso, D., Martin-Alfonso, M.J., Luckham, P.F., Martinez-Boza, F.J., 2019. Rheological characterisation of xanthan gum in brine solutions at high temperature. Carbohydr. Polym. 203, 103-109. https://doi.org/10.1016/j.carbpol.2018.09.034.

Reinoso, D., Martin-Alfonso, M.J., Luckham, P.F., Martinez-Boza, F.J., 2020. Flow behavior and thermal resistance of xanthan gum in formate brine. J Petrol. Sci Eng. 188, 106881. https://doi.org/10.1016/j.petrol.2019.106881.

Sulaimon, A.A., Adeyemi, B.J., Rahimi, M., 2017. Performance enhancement of selected vegetable oil as base fluid for drilling HPHT formation. J. Petrol. Sci. Eng. 152, 49–59. https://doi.org/10.1016/j.petrol.2020.107129.

Tapavicza, S.V., 2005. Vegetable esters make drilling fluids more environmentally friendly. Oil and Gas J. 103, 22.

Tartaglione, G., Tabuani, D., Camino, G., Moisio, M., 2008. PP and PBT composites filled with sepiolite: Morphology and thermal behaviour. Compos. Sci. Technol.68, 451–60. https://doi.org/10.1016/j.micromeso.2007.04.020.

Tiemblo, P., García, N., Hoyos, M., Mejía, A., de Francisco, R., 2015. Organic Modification of Hydroxylated Nanoparticles: Silica, Sepiolite, and Polysaccharides, in Handbook of Nanoparticles, M. Aliofkhazraei, Editor, Springer International Publishing. p. 1-35.

Weng, J., Gong, Z., Liao, L., Lv, G., Tan, J., 2018. Comparison of organo-sepiolite modified by different surfactants and their rheological behavior in oil-based drilling fluids. Appl. Clay Sci. 159, 94–101. https://doi.org/10.1016/j.clay.2017.12.03.

Wu, X.J., Wang, Y., Wang, M., Yang, W., Xie, B.H., Yang, M.B., 2012. Structure of fumed silica gels in dodecane: Enhanced network by oscillatory shear. Colloid Polym. Sci. 290, 151-161. http://dx.doi.org/10.1007/s00396-011-2535-4.

Zhuang G., Wu, H., Zhang, H., Zhang, Z., Zhang, X., Liao, L., 2017. Rheological properties of organo-palygorskite in oil-based drilling fluids aged at different temperatures. App. Clay Sci. 137. 50-58. http://dx.doi.org/10.1016/j.clay.2016.12.015.

Zhuang, G., Zhang, Z., Yang, H., Tan, J., 2018a. Structures and rheological properties of organo-sepiolite in oil-based drilling fluids. Appl. Clay Sci. 154, 43-51. https://doi.org/10.1016/j.clay.2017.12.048.

Zhuang, G., Zhang, Z., Chen, H., 2018b. Influence of the interaction between surfactants and sepiolite on the rheological properties and thermal stability of organo-sepiolite in oil-based drilling fluids. Microporous Mesoporous Mater. 272, 143-154. https://doi.org/10.1016/j.micromeso.2018.06.017.

Zhuang, G., Zhang, Z., Peng, S., Gao, J., Jaber, M., 2018c. Enhancing the rheological properties and thermal stability of oil-based drilling fluids by synergetic use of organo-montmorillonite and organo-sepiolite. Appl. Clay Sci. 161, 505-512. https://doi.org/10.1016/j.clay.2018.05.018

Zhuang, G., Zhang, Z., Jaber, M., 2019. Organoclays used as colloidal and rheological additives in oil-based drilling fluids: An overview. App. Clay Sci. 177, 63-81. https://doi.org/10.1016/j.clay.2019.05.006.